UDC 551.515.8:551.588.2:551.501.4.001.57

THE RESPONSE OF A MIDDLE-LATITUDE MODEL ATMOSPHERE TO FORCING BY TOPOGRAPHY AND STATIONARY HEAT SOURCES [1, 2]

JACQUES DEROME

Meteorological Service of Canada, Montreal, Quebec

A. WIIN-NIELSEN

Department of Meteorology and Oceanography, The University of Michigan, Ann Arbor, Mich.

ABSTRACT

The middle-latitude standing wave problem is investigated by means of a quasi-geostrophic, linear, steady-state model in which the zonal current is perturbed by the lower boundary topography and by a distribution of heat sources and sinks. All the perturbations are assumed to have a single meridional wavelength and the dissipation is considered to take place in the surface boundary layer using, as a first approach, a horizontally uniform drag coefficient.

After investigating some basic properties of the model atmosphere, some computations are made to determine its response to the combined forcing by topography and by diabatic heating for January 1962. The resulting perturbations are found to be in rather good agreement with the observed standing waves. The results also indicate that the standing waves forced by the topography are in about the same position as those forced by the diabatic heating and that the former have somewhat larger amplitudes than the latter.

The effect of allowing the drag coefficient to have one constant value over the continents and a smaller constant value over the oceans is examined and found to be quite important when the ratio of the two values is 6, but small (yet such as to bring the computed and observed eddies into closer agreement than in the case of a uniform drag coefficient) for a ratio of 2.

1. INTRODUCTION

One of the main problems encountered in the development of a general theory of climates is explaining how the large-scale atmospheric standing waves are maintained against the dissipative forces. It is the purpose of this paper to examine this problem using a steady-state, two-level, quasi-geostrophic model of the atmosphere in which the standing waves are forced both by the earth's topography as obtained from Berkofsky and Bertoni (1955) and by a steady distribution of heat sources and sinks obtained from Brown (1964). The approach used here falls within the scope of the second of the two approaches to the standing wave problem discussed by Saltzman (1968). In the first approach, general circulation experiments are performed (i.e., the atmospheric model equations are integrated numerically over relatively long periods of time using various values of the external parameters in such a way that their effects on the solution can be determined). It is then possible to examine how the various physical mechanisms included in the model contribute to bring about the standing eddy component of the computed climate, the latter being defined as the zonally asymmetric part of the time-averaged solution of the model. Numerical general circulation models including forcing mechanisms for the standing waves have been presented (e.g., Mintz 1965 and Miyakoda et al. 1969). The results of these studies are encouraging but in view of the complexity of the problem, it is useful to supplement the above approach with a second one.

In the second approach, the procedure is to solve the model equations relating the time-averaged variables themselves to the time-averaged distribution of heat and momentum sources due to diabatic processes, topography, friction, and transient disturbances (cf. Saltzman 1961). On the grounds that the amplitudes of the standing eddy components are small compared to their respective zonal mean counterparts, the nonlinear equations are usually approximated by linear perturbation equations in which the zonal mean variables are assumed to be known from observations. As for the sources of heat and momentum, they can be either specified or parameterized in terms of the time-averaged variables themselves. The choice made by previous investigators and their main modeling assumptions have been reviewed by Saltzman (1968).

The present study extends the work of authors who considered the forcing of stationary waves by either topography (e.g., Charney and Eliassen 1949, Bolin 1950, Gambo 1956, Murakami 1963, Sankar-Rao 1965*a*) or diabatic heating (e.g., Smagorinsky 1953, Gilchrist 1954, Döös 1962, Sankar-Rao 1965*c*, Sankar-Rao and Saltzman 1969) in that here both mechanisms are included in the same model. In this sense, it is similar to the investigations of the Staff Members, Academia Sinica (1958), Saltzman (1965), and Sankar-Rao (1965*b*). Our treatment of the diabatic effects differs from the previous ones, however, in that we use a time-averaged distribution of heat sources and sinks computed by Brown (loc. cit.) from daily atmospheric data for January 1962. In earlier studies, the diabatic heating fields were generally either parameterized or prescribed as a simple harmonic function of the spatial coordinates. One exception is the investiga-

[1] Based in part on a thesis submitted by the first author as partial fulfillment of the requirements for the Ph. D. degree at The University of Michigan

[2] Publication No. 185 from the Department of Meteorology and Oceanography, The University of Michigan

tion by the Staff Members, Academia Sinica (loc. cit.), in which the heating fields were obtained from atmospheric data; but since rather restrictive assumptions were made both in the computation of the heating fields and in the modeling of the stationary waves, there is a need for a further examination of the problem.

2. THE STEADY STATE QUASI-GEOSTROPHIC MODEL

We shall assume that the motion takes place on a β plane centered at 45°N so that we can use a Cartesian coordinate system in which the x and y coordinates increase to the east and north, respectively; and we shall make use of the hydrostatic approximation to introduce pressure as the vertical coordinate. The steady state quasi-geostrophic vorticity and thermodynamic equations then take the form

$$\mathbf{V}\cdot\nabla(\zeta+f)=f_0\frac{\partial\omega}{\partial p} \tag{1}$$

and

$$\mathbf{V}\cdot\nabla\left(\frac{\partial\phi}{\partial p}\right)+\sigma\omega=-\frac{RH}{c_p p}, \tag{2}$$

respectively (Wiin-Nielsen 1959). In the above, $\mathbf{V}$ is the nondivergent part of the horizontal velocity vector, with components u and v along the x and y axes, respectively; ζ is the vertical component of relative vorticity; f is the Coriolis parameter with value f_0 at 45°N; ω is the vertical velocity dp/dt where p is the pressure and t is time; $g=9.8\ \mathrm{m\cdot s^{-2}}$ is the acceleration of gravity; $\nabla=\mathbf{i}\partial/\partial x+\mathbf{j}\partial/\partial y$, where $\mathbf{i}$ and $\mathbf{j}$ are unit vectors pointing to the east and north, respectively; $\phi=gz$ where z is the height above mean sea level; $\sigma=-\alpha\partial\ \ln\theta/\partial p$ is the static stability parameter in which α is the specific volume and θ is potential temperature; $R=0.287\ \mathrm{kJ\cdot kg^{-1}\cdot deg^{-1}}$ is the gas constant for air; $c_p=1.004\ \mathrm{kJ\cdot kg^{-1}\cdot deg^{-1}}$ is the specific heat at constant pressure; and H is the diabatic heating per unit time and unit mass. In this formulation, σ is independent of the horizontal coordinates (Phillips 1963). The friction terms do not appear explicitly in eq (1) and (2), but the effect of friction will be taken into account through the lower boundary condition in the manner suggested by Charney and Eliassen (1949), that is, by considering that friction in the Ekman boundary layer introduces some vertical motion at the bottom of the free atmosphere.

In eq (2), we shall take H to be a known function and introduce the approximation

$$\phi=f_0\Psi. \tag{3}$$

The nature of this last approximation has been discussed by Phillips (1958).

For our modeling assumption to be as consistent as possible with those used by Brown (loc. cit.) to compute the heating fields, we shall follow the latter in using a two-level representation of the atmosphere. When one uses the integers 0, 1, 2, 3, and 4 as subscripts to represent the values of any variable at the pressure levels $p=0$, 25, 50, 75, and 100 cb, respectively, and introduces the notation

$$(\ )_*=1/2[(\ )_1+(\ )_3] \tag{4}$$

and

$$(\ )_T=1/2[(\ )_1-(\ )_3], \tag{5}$$

eq (1), (2), and (3) can be cast into the form

$$\mathbf{V}_*\cdot\nabla(\zeta_*+f)+\mathbf{V}_T\cdot\nabla\zeta_T=\frac{f_0}{p_4}\omega_4, \tag{6}$$

$$\mathbf{V}_*\cdot\nabla\zeta_T+\mathbf{V}_T\cdot\nabla(\zeta_*+f)=\frac{f_0}{p_2}\omega_2-\frac{f_0}{p_4}\omega_4, \tag{7}$$

and

$$2f_0\mathbf{V}_*\cdot\nabla\Psi_T-\sigma_2 p_2\omega_2=\frac{R}{c_p}H \tag{8}$$

after some elementary manipulations. In deriving eq (6), (7), and (8), the derivatives with respect to pressure have been replaced by finite differences; and the boundary condition $\omega_0=0$ has been used. The lower boundary condition will be taken to be

$$\omega_4=\mathbf{V}_4\cdot\nabla p_g-\frac{p_4F}{2f_0}\zeta_4, \tag{9}$$

the first contribution to ω_4 being due to the flow of air over uneven terrain where the standard pressure is p_g and the second contribution resulting from the viscosity in the Ekman layer (e.g., Charney and Eliassen 1949, Phillips 1956, and Wiin-Nielsen 1961). In the sequel, the quantity F in eq (9) will be called the "friction coefficient." While most results presented in this paper were obtained with F treated as a constant, some results will also be shown for which F was taken to be larger over the continents than over the oceans.

To obtain the vorticity and nondivergent wind at 100 cb appearing in eq (9), we follow Smagorinsky (1963, p. 164) and extrapolate the geopotential (which here is the same as extrapolating the stream function) from 25 and 75 cb to 100 cb on the assumption of a constant temperature lapse rate of 6.5°C/km. Upon integrating the hydrostatic equation, we then obtain

$$\Psi_4=\Psi_*-1.6\Psi_T. \tag{10}$$

Using the same procedure, one can derive the relation

$$\Psi_2=\Psi_*-0.2\Psi_T, \tag{11}$$

which is a relation used only for display purposes, that is, to obtain Ψ_2 for comparison with observations once Ψ_* and Ψ_T have been obtained from the model equations.

We now linearize eq (6–9) by considering that the flow consists of a zonal component on which small-amplitude perturbations are superimposed. The former is characterized by the stream functions $-U_*y$, $-U_Ty$, and the latter by the stream functions ψ_* and ψ_T forced by the perturbation heating H and variations in ground pressure

p_g. The linearized versions of eq (6–9), after elimination of the vertical velocity, then take the form

$$\left(U_*\frac{\partial}{\partial x}\nabla^2+\frac{F}{2}\nabla^2+\beta\frac{\partial}{\partial x}\right)\psi_*+\left(U_T\frac{\partial}{\partial x}\nabla^2-0.8\,F\nabla^2\right)\psi_T=\frac{f_0}{p_4}\left(U_*-1.6\,U_T\right)\frac{\partial p_g}{\partial x} \quad (12)$$

and

$$\left(U_T\frac{\partial}{\partial x}\nabla^2-\frac{F}{2}\nabla^2+\delta^2U_T\frac{\partial}{\partial x}\right)\psi_*+\left[U_*\frac{\partial}{\partial x}\nabla^2+0.8\,F\nabla^2+(\beta-U_*\delta^2)\frac{\partial}{\partial x}\right]\psi_T=-\frac{4Rf_0}{c_p\sigma_2p_4^2}H-\frac{f_0}{p_4}(U_*-1.6\,U_T)\frac{\partial p_g}{\partial x} \quad (13)$$

where

$$\delta^2=\frac{8f_0^2}{\sigma_2p_4^2}$$

and

$$\beta=df/dy=\text{const}\qquad(16\times10^{-12}\text{m}^{-1}\cdot\text{s}^{-1}).$$

In the following, we shall assume that the perturbation quantities have a simple meridional structure given by $\cos(\mu y)$, that is,

$$[\psi_*,\psi_T,H,p_g]=[\hat{\psi}_*(x),\hat{\psi}_T(x),\hat{H}(x),\hat{p}_g(x)]\cos(\mu y) \quad (14)$$

in which we take $y=0$ at 45°N so that the perturbation quantities have a maximum absolute value there. Equation (14) is a solution to eq (12) and (13) if U_* and U_T are constants. This assumption is made throughout the paper except for the experiment mentioned at the end of subsection 5A. Charney and Eliassen (1949) evaluated from an inspection of the main mountain barriers that the meridional wavelength $L_y=2\pi/\mu$ should be approximately 50° of latitude. They found, on the other hand, that their model for the standing waves forced by the topography yielded standing waves which closely approximated the observed ones when L_y was assumed to be 66° of latitude. Smagorinsky (1953) used two separate values of the meridional wavelength in his study of standing waves forced by diabatic heating, namely, 35.0° and 53.9° of latitude. In the present study, the meridional wavelength will be taken to be 60° of latitude ($\mu=0.95\times10^{-6}$ m^{-1}) for most computations.

The longitudinal dependence of the perturbations will be represented by the Fourier series

$$[\hat{\psi}_*(\lambda),\hat{\psi}_T(\lambda),\hat{H}(\lambda),\hat{p}_g(\lambda)]=\sum_{n=1}^{N}\{[A_n^*,A_n^T,Q_n,R_n]\times\cos(n\lambda)+[B_n^*,B_n^T,T_n,S_n]\sin(n\lambda)\} \quad (15)$$

in which $\lambda=x/a\cos\varphi_0$ is the longitude, a and φ_0 being the radius of the earth and 45°N, respectively. When eq (14) and (15) are substituted in eq (12) and (13), the following system of algebraic equations is obtained:

$$\begin{bmatrix}a_1 & -a_2 & -1.6\,a_1 & a_3\\ a_2 & a_1 & -a_3 & -1.6\,a_1\\ a_1 & a_4 & -1.6\,a_1 & a_5\\ a_4 & -a_1 & -a_5 & 1.6\,a_1\end{bmatrix}\begin{bmatrix}A_n^*\\ B_n^*\\ A_n^T\\ B_n^T\end{bmatrix}=\begin{bmatrix}-bS_n\\ bR_n\\ -bS_n-qQ_n\\ -bR_n+qT_n\end{bmatrix} \quad (16)$$

where

$$a_1=FK^2a\cos\varphi_0/2n,$$
$$a_2=\beta-K^2U_*,$$
$$a_3=K^2U_T,$$
$$a_4=U_T(\delta^2-K^2),$$
$$a_5=\beta-U_*(\delta^2+K^2),$$
$$b=\frac{f_0}{p_4}(U_*-1.6\,U_T),$$
$$q=\frac{4Rf_0a\cos\varphi_0}{\sigma_2c_pp_4^2n},$$

and

$$K^2=\left(\frac{n}{a\cos\varphi_0}\right)^2+\mu^2.$$

If S_n, R_n, Q_n, and T_n are considered known from observations, eq (16) can be solved for A_n^*, B_n^*, A_n^T, B_n^T for $1\leq n\leq N$. Then $\hat{\psi}_*$ and $\hat{\psi}_T$ can be obtained from eq (15); and $\hat{\psi}_1$, $\hat{\psi}_2$, and $\hat{\psi}_3$, from eq (4), (5), and (11).

To get some insight into the basic properties of the two-level model, we shall first compute the response of the model to forcing by either the bottom topography or by the diabatic heating. The attention will be focused in the next sections on changes in the model properties with the zonal wavelength of the disturbance.

3. RESPONSE TO TOPOGRAPHIC FORCING

We shall consider the adiabatic flow of the model atmosphere over a surface where the standard pressure is given by a simple harmonic function with an amplitude of 1 cb, that is

$$\hat{p}_g(\lambda)=\cos(n\lambda), \quad (17)$$

and solve eq (16) for $n=1, 2, \ldots, N$. The solution for the mean stream function will be written in the form

$$\hat{\psi}_*(\lambda)=C_n^*\cos(n\lambda-\alpha_n^*) \quad (18)$$

where

$$C_n^*=(A_n^{*2}+B_n^{*2})^{1/2} \quad (19)$$

and

$$\alpha_n^*=\tan^{-1}(B_n^*/A_n^*) \quad (20)$$

with similar expressions for the thermal stream function.

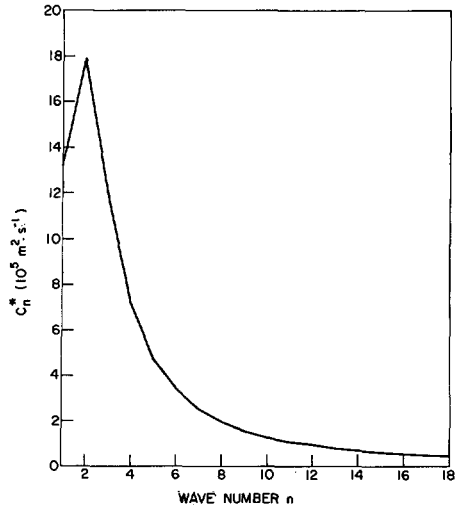

FIGURE 1.—Amplitude of the mean stream function forced by a sinusoidal distribution of $\hat{p}_g$ with zonal wave number n and an amplitude of 1 cb. The parameters are $U_*=15$ m/s, $U_T=5$ m/s, $F=4\times10^{-6}$ s^{-1}, and $\mu^2=0.90\times10^{-12}$ m^{-2} (i.e., $L_y=60°$ of lat.).

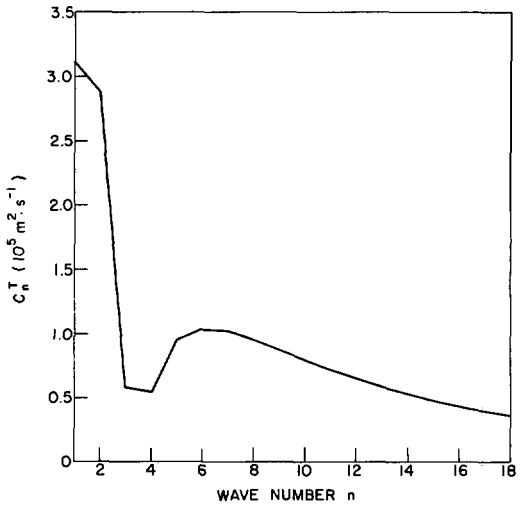

FIGURE 2.—Amplitude of the thermal stream function forced by a sinusoidal distribution of $\hat{p}_g$ with zonal wave number n and an amplitude of 1 cb. The parameters are the same as those in figure 1.

In all the computations, the parameters were assigned the following values representative of winter conditions:

$$F=4\times10^{-6}\ \text{s}^{-1},\ U_*=15\ \text{m/s},\ U_T=5\ \text{m/s},$$

$$\sigma_2=3\times10^{-6}\ \text{m}^4\cdot\text{s}^2\cdot\text{kg}^{-2},\ \text{and}\ \mu^2=0.9\times10^{-12}\text{m}^{-2}$$

(corresponding to a meridional wavelength of 60°).

The plot of C_n^* appears in figure 1 as a function of the zonal wave number n. We note that the amplitude of the ψ_* wave is largest for $n=2$ and decreases rather rapidly as n changes, indicating that the model atmosphere is more easily excited on the scale of the wave with $n=2$ than on any other scale. For example, we see that the amplitude of the wave is approximately 15 times larger for $n=2$ than for $n=10$. The model is, therefore, relatively insensitive, at least with respect to the mean stream function, to the presence of the high wave number components in the expansion eq (15) for $\hat{p}_g(\lambda)$.

The reason for the maximum response at $n=2$ is made clear by an analysis of the time-dependent analog of eq (12) and (13) without forcing mechanisms. The analysis reveals that, in the special case where $F=U_T=0$, the time-dependent model has two normal modes of oscillation with phase speeds of

$$c=U_*-\beta/K^2 \tag{21}$$

for the nondivergent mode, for which $\psi_T\equiv0$, $\psi_*\not\equiv0$, and

$$c=U_*-\beta/(K^2+\delta^2) \tag{22}$$

for the divergent mode, for which $\psi_*\equiv0$, $\psi_T\not\equiv0$ (Thompson 1961, pp. 110–112). For the parameters used above, we find that eq (21) yields $c=0$ for $n=1.82$. This implies that, at $n=2$, the nondivergent mode has a nearly vanishing frequency, leading to a condition of quasi-resonance in the forced problem due to a forcing mechanism operating at nearly the same frequency as one of the natural frequencies of the system. In our model, pure resonance does not occur because a dissipation mechanism has been incorporated (in addition to the fact that only integral values of n are possible); but the largest response is nevertheless obtained near the resonance point of the inviscid problem. It should also be kept in mind that, in our model, $U_T\neq0$ [as opposed to eq (21) and (22)] and that the effects of vertical wind shear should be considered in a more detailed discussion.

Some computions have also been made using a meridional wavelength of 100° of latitude ($\mu^2=0.324\times10^{-12}$ m^{-2}), in which case the perturbations have a maximum amplitude at 45°N and vanish at 20°N and 70°N. According to eq (21), the nondivergent mode would be stationary for $n=3.9$; hence, we would expect quasi-resonance in the topographically forced model (with $F=U_T=0$ at $n=4$) since only integral values of n are admissible. The computations have shown that, with F and U_T as in figure 1, the amplitude of the mean stream function forced by a 1-cb oscillation in $\hat{p}_g$ does, indeed, rise from a value of $7.8\times10^5\cdot\text{m}^2\cdot\text{s}^{-1}$ at $n=1$ to a maximum value of $28.6\times10^5\cdot\text{m}^2\cdot\text{s}^{-1}$ at $n=4$ and then decreases monotonically as n increases.

From eq (22), we find that, in the case $U_T=F=0$ and for the values of the other parameters listed above, no value of K exists for which $c=0$; thus in this case, no divergent mode ($\psi_*\equiv0$, $\psi_T\not\equiv0$) could be made to resonate by a steady-state forcing mechanism—in contrast to the nondivergent modes. It would seem reasonable to expect, then, that this property would be reflected in the model having nonvanishing U_T and F by a weaker response in ψ_T than in ψ_* to a simple harmonic mountain, at least in the parameter-space vicintiy of the quasi-resonance point for ψ_*. This can be seen to be the case by comparing figure 2, which gives the amplitude of the ψ_T wave forced

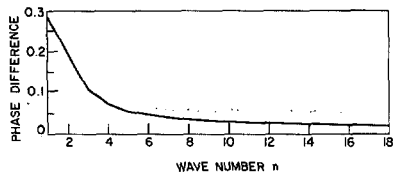

FIGURE 3.—Phase difference between zonal wave number n in the mean stream function and the same harmonic in the function $-\hat{p}_g$. The mean stream function wave is to the west of the $-\hat{p}_g$ wave by the fraction of the zonal wavelength indicated in the ordinate. The parameters are the same as those in figure 1.

by a 1-cb oscillation in p_g as a function of the zonal wave number, with figure 1. We note that, for zonal wave number 2, the amplitude of the ψ_T wave is 6.2 times smaller than that of the ψ_* wave, in agreement with the above discussion.

Since the thermal stream function ψ_T is proportional to mean temperature between 25 and 75 cb, we can think of figure 2 as giving the amplitude of that temperature wave near 50 cb that is forced by a 1-cb oscillation in $\hat{p}_g$. We see that the amplitude of this temperature wave has a maximum amplitude for $n=1$ and a relative minimum near zonal wave numbers 3 and 4. The latter coincides with the region of the spectrum where the computations reveal a radical change in the phase relationship between the ψ_* and ψ_T waves in the sense that the mean and thermal stream functions are exactly in phase for $n=1$, 2, and 3 and out of phase by exactly half a wavelength for $n\geq 4$.

To gain some insight into this behavior, we return again to the simplified model with $F=U_T=0$. In this case, we find from eq (13), using the same values of the other parameters as above, that the $\hat{\psi}_T$ and $\hat{p}_g$ waves are exactly in phase with each other so that, near 50 cb, the low temperatures would be found over the terrain ridges and the high temperatures would be found over the terrain troughs. (This phase relationship would be different if the mean zonal wind were sufficiently small and/or the static stability were sufficiently large. Resonance in the ψ_T field would then also become possible.) From eq (12), on the other hand, we find that the resonance point where

$$K^2=\beta/U_*=K_R^2$$

separates the region where the $\hat{\psi}_*$ and $\hat{p}_g$ waves are exactly in phase with each other ($K < K_R$) from the region where they are half a wavelength out of phase ($K > K_R$). In short, on the longwave side of the resonance point K_R, the mean and thermal stream functions are in phase with each other and with the $\hat{p}_g$ wave; on the shortwave side of K_R, on the other hand, the mean and thermal stream functions are half a wavelength out of phase with each other, the latter being in phase with the $\hat{p}_g$ wave. We note that the above phase relationships imply that the amplitude of the stream function wave increases or decreases with height depending on whether K is on the longwave or shortwave side of K_R, respectively. We shall see in subsection 5B that, even in the case $U_T\neq 0$ and F is an arbitrary function of longitude, the topographically forced mean and thermal stream functions are either exactly in phase or half a wavelength out of phase with each other. The position of these waves relative to the topography does depend, however, on the values of U_T and F.

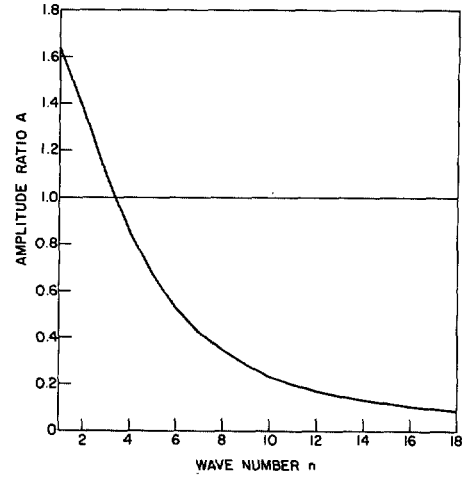

FIGURE 4.—Amplitude ratio of the stream function forced by a sinusoidal distribution of $\hat{p}_g$ with zonal wave number n. The parameters are the same as those in figure 1.

The influence of the mean thermal wind and friction on the phase of the forced perturbations can be seen by comparing the results of the above discussion with those of figure 3, which gives the phase difference (as a fraction of a wavelength) between the trough in the $\hat{p}_g$ wave (or the ridge in the terrain elevation) and the first upstream ridge in the $\hat{\psi}_*$ wave for the case $U_T=5$ m/s, $F=4\times10^{-6}$ s^{-1}. For example, we see that, for zonal wave number 2, the ridge in the ψ_* wave is about one-fifth of a wavelength upstream from the trough in the $\hat{p}_g$ wave. It is clear that, for all zonal wave numbers, the ridge in the $\hat{\psi}_*$ wave tends to be to the west of the ridge in the terrain height and that this displacement decreases as the zonal wave number increases. As mentioned above, for $n = 1$, 2, and 3, the thermal stream function wave is exactly in phase with the mean stream function; whereas for $n \geq 4$, these two waves are half a wavelength out of phase. We come to the conclusion, as has Saltzman (1965), that the topographically forced perturbations have no tilt with height and, therefore, cannot transport heat in the meridional direction.

As a measure of the amplification or damping with height, we shall use the ratio of the amplitude of the $\hat{\psi}_1$ wave to that of the $\hat{\psi}_3$ wave. This ratio, denoted by A, appears in figure 4 as a function of the zonal wave number. We find that those components with $n=1$, 2, and 3 amplify while the others damp with height, in accordance with the phase relationships obtained above. It will be shown in subsection 5B that the amplitude ratio A is independent of the friction coefficient F, even when the latter is assumed to be a function of longitude.

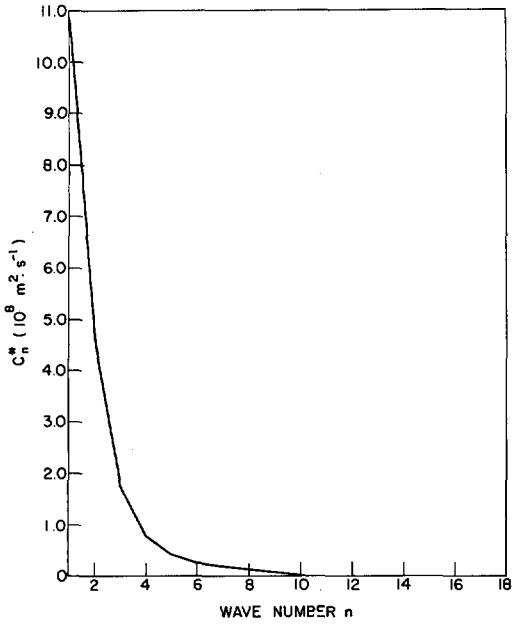

FIGURE 5.—Amplitude of the mean stream function forced by a sinusoidal distribution of $\hat{H}$ with zonal wave number n and an amplitude of 10^{-3} kJ·kg^{-1}·s^{-1}. The parameters are the same as those in figure 1.

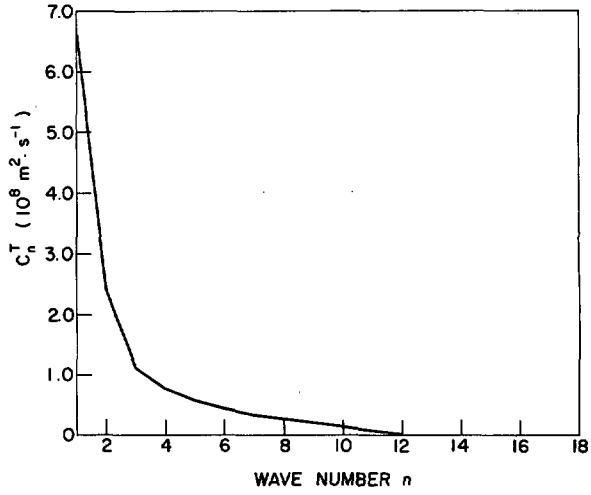

FIGURE 6.—Amplitude of the thermal stream function forced by a sinusoidal distribution of $\hat{H}$ with zonal wave number n and an amplitude of 10^{-1} kJ·kg^{-1}·s^{-1}. The parameters are the same as those in figure 1.

4. RESPONSE TO FORCING BY HEAT SOURCES AND SINKS

The discussion of this section is similar to that of the previous one except that here the standing waves are produced by the diabatic heating. We shall, therefore, set $p_g \equiv 0$, obtaining

$$\hat{H}(\lambda) = Q_n \cos(n\lambda) \tag{23}$$

with $Q_n = 10^{-3}$ kJ·kg^{-1}·s^{-1}, and solve the system, eq (16). The response can then be written in the form of eq (18), (19), and (20) for the mean stream function; similar expressions can be written for the thermal stream function.

The amplitude C_n^* of the mean stream function appears as a function of the zonal wave number in figure 5. We see that, contrary to the case where the perturbations result from the presence of the topography (fig. 1), the most easily excited mode here is zonal wave number 1. The decrease in C_n^* as n increases is seen to be quite rapid. In fact, C_4^* is less than 10 percent of C_1^*; and C_{10}^* is again less than 10 percent of C_4^*.

The amplitude C_n^T of the thermal stream function can be seen in figure 6 as a function of the zonal wave number. Just as in the case of the mean stream function, zonal wave number 1 is found to be the most easily excited mode.

We note that, in the case under discussion, the solution to eq (16) can be written explicitly as

$$A_n^* + iB_n^* = qQ_n\Delta^{-2}\{a_1[a_3(1.6\,a_2 - a_3 + a_5) - 1.6\,a_2a_5] + i[1.6\,a_1^2(a_3 - 1.6\,a_2 - 1.6\,a_4 - a_5) - a_3(a_2a_5 + a_3a_4)]\} \tag{24}$$

and

$$A_n^T + iB_n^T = qQ_n\Delta^{-2}\{a_1[a_2(1.6\,a_2 + 1.6\,a_4 - a_3) - a_3a_4] + i[a_1^2(a_3 - 1.6\,a_2 - 1.6\,a_4 - a_5) - a_2(a_2a_5 + a_3a_4)]\} \tag{25}$$

where

$$\Delta^2 = (a_2a_5 + a_3a_4)^2 + a_1^2(a_3 - 1.6\,a_2 - 1.6\,a_4 - a_5)^2.$$

Here, $i = \sqrt{-1}$ and the a_i's have been defined after eq (16). Since a_1 is proportional to the friction coefficient, F, we find that, in the frictionless case, $A_n^* = A_n^T = 0$,

$$B_n^* = -\frac{qQ_na_3}{a_2a_5 + a_3a_4}, \tag{26}$$

and

$$B_n^T = -\frac{qQ_na_2}{a_2a_5 + a_3a_4}. \tag{27}$$

Thus the amplitude of the mean stream function goes to zero as the vertical wind shear vanishes ($a_3 = 0$), while that of the thermal stream function tends to become inversely proportional to a_5, that is, to $[\beta - U_*(\delta^2 + K^2)]$. The resonance in the thermal mode then occurs if there is a real value of K that makes this factor zero (this is not the case for the values of the parameters used in this study). We see also from eq (26) and (27) that since

$$B_n^* = \frac{a_3}{a_2}B_n^T = \frac{K^2U_TB_n^T}{\beta - K^2U_*}, \tag{28}$$

the mean and thermal stream functions are in phase with each other on the longwave side of the point $K^2 = \beta/U_*$ in which case the amplitude of the stream-function wave increases with height. On the shortwave side of this point, on the other hand, the mean and thermal stream functions are a half wavelength out of phase with each other; and the amplitude of the stream-function wave decreases with

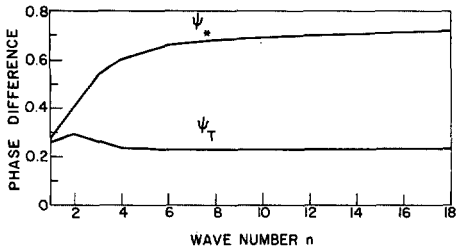

FIGURE 7.—Phase difference between zonal wave number n in the function $\hat{H}$ and the same harmonic in the mean (upper curve) or thermal (lower curve) stream function. The stream function waves are to the east of the $\hat{H}$ wave by the fraction of the zonal wavelength indicated on the ordinate. The parameters are the same as those in figure 1.

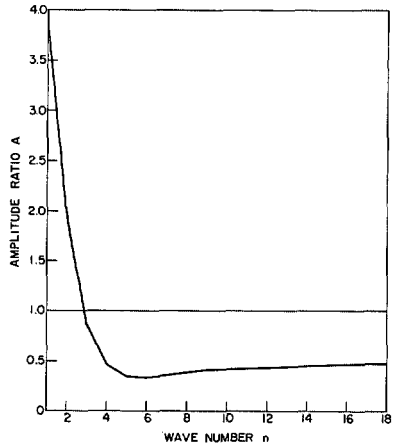

FIGURE 8.—Amplitude ratio of the stream function forced by a sinusoidal distribution of $\hat{H}$ with zonal wave number n. The parameters are the same as those in figure 1.

height. We emphasize here that these conclusions are valid only for the case $F=0$.

The phase lag between the various harmonics in the heating function H and the corresponding harmonics in the mean and thermal stream functions for the case $F=4\times10^{-6}\,s^{-1}$ can be seen in figure 7. The phase difference is defined here as the distance, in units of the zonal wavelength determined by n, between a ridge in the forcing function $\hat{H}$ and the first ridge downstream in the response $\hat{\psi}_*$ and $\hat{\psi}_T$. Thus we observe that, for zonal wave number 2, the ridges in the mean stream function are about 0.42 of one wavelength downstream from the ridges in the heating function, that is, the ridges (troughs) in the mean stream function occur only slightly to the west of the longitudes of maximum cooling (heating). For the same harmonic, the thermal stream function is seen to be about 0.13 of one wavelength to the west of the mean stream function so that the stream function slopes to the west with height and therefore transports heat northward. This is in qualitative agreement with the results obtained by Saltzman (1965) and previously by Smagorinsky (1953), using a zonal wavelength of 160° of longitude and a meridional wavelength of 53.9° of latitude (ours is 60°).

The amplitude ratio A as defined in the previous section appears in figure 8. We see that wave components 1 and 2 amplify with height, whereas the others damp with height. We note that this is in agreement with the inviscid case discussed after eq (28). It is interesting to compare these results with those shown in figure 4 where the standing waves are maintained by the topography. We see, for example, that the amplitude of the stream function for $n=1$ increases by a factor of about 3.9 between 75 cb and 25 cb when the wave is created by the diabatic heating (fig. 8), whereas it increases by only a factor of about 1.6 when the wave is due to topographic effects (fig. 4). This seems to be in part a reflection of the fact that, in the present model, the topographic forcing tends to place, at least for the long waves, most of the energy in the mean mode; whereas the internal diabatic heating tends to partition the energy somewhat more evenly between the mean and thermal modes.

5. THE RESPONSE OF THE TWO-LEVEL MODEL TO THE TOPOGRAPHY AND DIABATIC HEATING NEAR 45°N

A. CASE OF A CONSTANT FRICTION COEFFICIENT

In an attempt to see whether or not the model presented in the previous section is capable of reproducing the main features of the observed standing waves, we have determined the solution that it yields when p_g is obtained (using a standard atmosphere) from the ground height values published by Berkofsky and Bertoni (1955) and $\hat{H}$ is taken from the computations by Brown (1964) for January 1962. The values of U_* and U_T were taken to be 15 m/s and 5 m/s, respectively, so as to be representative of the middle-latitude conditions in January, the month for which the values of the diabatic heating apply. The computations were made for a few values of the friction coefficient F and the meridional wave number μ.

In view of the simple meridional structure that we assume for the perturbations [see eq (14)], we need, strictly speaking, to know $\hat{p}_g$ and $\hat{H}$ along one latitude circle only, say 45°N. To introduce some smoothing, on the other hand, we assumed $\hat{p}_g(\lambda)$ and $\hat{H}(\lambda)$ to be the meridional averages of the standard pressure at the ground and of the heating between 30°N and 60°N. The Fourier coefficients appearing in the expansion [eq (15)] for $p_g(\lambda)$ were then computed from the relations

$$[R_n, S_n]=\frac{1}{\pi}\int_0^{2\pi}\hat{p}_g(\lambda)[\cos(n\lambda), \sin(n\lambda)]d\lambda \qquad (29)$$

with analogous relations holding true for the Fourier coefficients Q_n and T_n in the expansion of $\hat{H}(\lambda)$. The integrals in eq (29) were evaluated numerically using intervals of 5° of longitude. The amplitude and phase of zonal wave components 1 through 18 for the standard pressure

TABLE 1.—*Mean amplitude and phase of the standard pressure and diabatic heating between 30°N and 60°N for zonal wave numbers 1 through 18*

Zonal wave Number n	Standard pressure		Diabatic heating	
	$(R_n^2+S_n^2)^{1/2}$	$\tan^{-1}(R_n/S_n)$	$(Q_n^2+T_n^2)^{1/2}$	$\tan^{-1}(Q_n/T_n)$
	(cb)	(deg.)	(10^{-6} kJ·kg^{-1}·s^{-1})	(deg.)
1	4.22	183.2	4.95	216.9
2	5.21	107.2	9.21	153.0
3	2.71	310.7	2.16	181.9
4	2.34	279.6	4.71	227.1
5	2.28	156.4	1.53	122.9
6	0.59	130.1	3.45	303.4
7	1.75	331.7	1.41	100.5
8	0.35	244.2	3.62	193.8
9	1.23	192.5	3.23	335.2
10	0.45	302.8	2.14	85.3
11	0.28	11.2	1.15	66.7
12	0.43	132.6	3.32	187.0
13	0.17	278.2	2.17	245.4
14	0.31	346.1	2.45	332.2
15	0.12	4.6	2.14	70.3
16	0.25	240.3	0.23	59.2
17	0.24	10.9	0.16	170.7
18	0.37	334.8	0.07	288.4
Zonal mean	96.08		2.51	

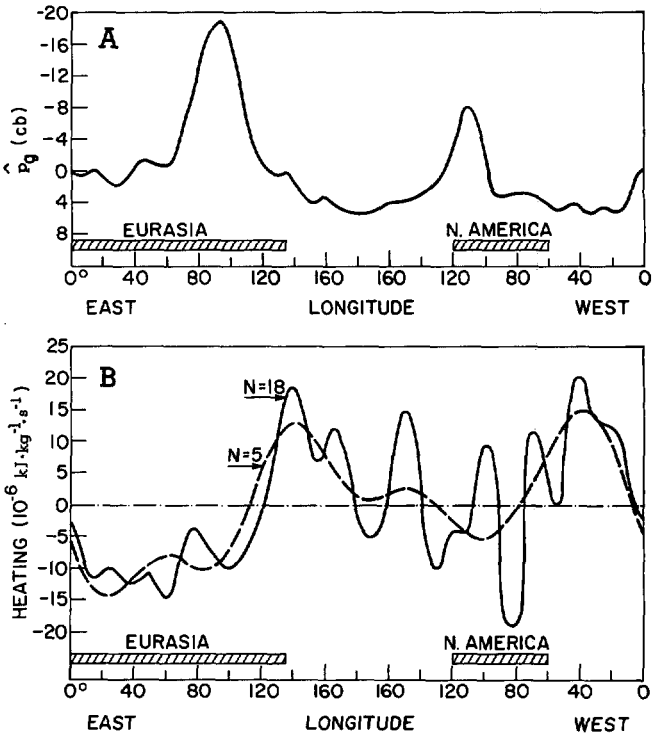

FIGURE 9.—(A) the function $\hat{p}_g$ as obtained from the first 18 zonal harmonics ($n=0$ excluded) of the mean standard pressure at the ground between 30°N and 60°N; the positions of the continents are shown schematically; (B) the diabatic heating function $\hat{H}$ as reconstructed from the first five and 18 zonal components ($n=0$ excluded) of Brown's (1964) heating values between 30°N and 60°N for January 1962.

at the ground and the diabatic heating (together with the zonal mean values) are given in table 1. We note in particular that, in both the topography and the diabatic heating, the maximum amplitude is found in zonal wave number 2 followed by wave number 1.

The function $\hat{p}_g(\lambda)$ as reconstructed from eq (15) using $N=18$ appears in figure 9A, and the reconstructed function $\hat{H}(\lambda)$ using $N=5$ and $N=18$ is given in figure 9B. It is clear from the dashed curve in figure 9B that the smoothed representation of Brown's (1964) heating has the tendency to be positive over the oceans (with the maximum occurring near the western edge of the oceans) and negative over the continents, as expected for the month of January.

To determine the importance of the topography in creating standing waves in our model atmosphere, first we consider the case in which $H\equiv 0$ and $\hat{p}_g$ is as shown in figure 9A. With the use of eq (16), (15) with $N=18$, and eq (4), (5), and (11), the forced perturbation heights at 25, 50, and 75 cb shown in figure 10 are obtained. At the three levels, the forced pattern consists of a major trough near 140°E, a ridge near 120°W, and a trough near 70°W. If we refer to figure 9A, we observe that the major trough at 140°E in figure 10 occurs in the lee of the Himalayas and nearly coincides with the eastern coast of Asia. We note also that the trough deepens by about 55 m and shifts by 5° to the east from 75 cb to 25 cb. Near the west coast of North America, we find a ridge that slopes from 120°W at 75 cb to 125°W at 25 cb. The second major trough appears near 65°W at the three pressure levels, that is, near the eastern coast of North America.

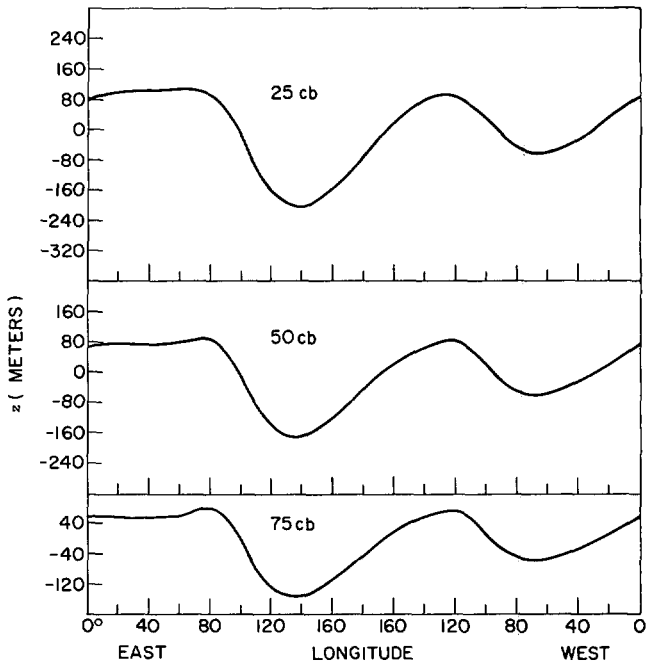

FIGURE 10.—Perturbation heights of the 25-, 50-, and 75-cb surfaces produced by the flow of the zonal current over the distribution of standard pressure at the ground shown in figure 9A. The parameters are the same as those in figure 1.

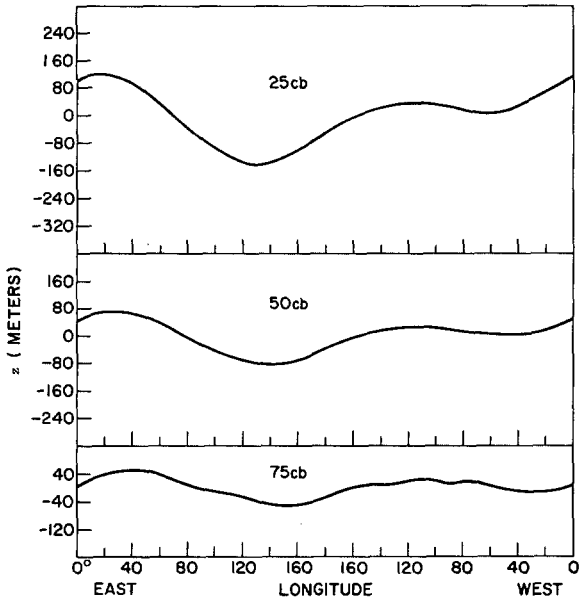

FIGURE 11.—Perturbation heights of the 25-, 50-, and 75-cb surfaces produced by the distribution of diabatic heating and cooling given by the solid curve in figure 9B. The parameters are the same as those in figure 1.

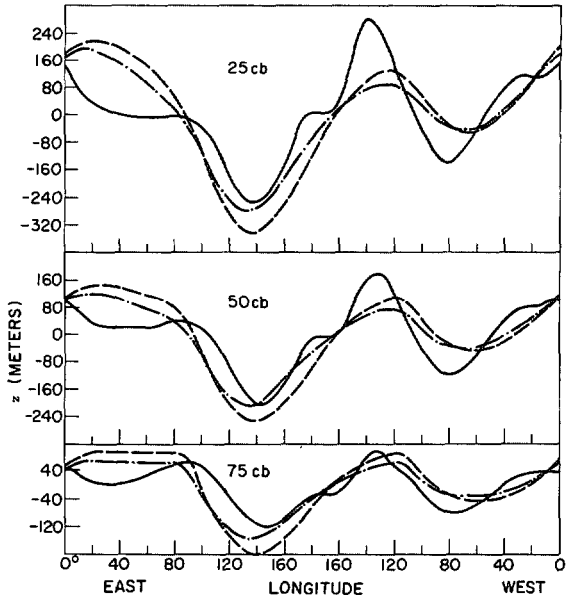

FIGURE 12.—Perturbation heights of the 25-, 50-, and 75-cb surfaces. The solid curves give the observed distribution for January 1962, as averaged between 30°N and 60°N. The dashed and dot-dashed curves show the response of the model to the combined forcing by the topography and diabatic heating (with $N=18$) using $F=4\times10^{-6}$ s^{-1} and $F=6\times10^{-6}$ s^{-1}, respectively. The other parameters are the same as those in figure 1.

The response of the model to the diabatic heating alone (solid curve, fig. 9B) appears in figure 11. Again, we find that the most prominent feature in the response is a trough near the eastern edge of Asia. The trough is about three times deeper at 25 cb than at 75 cb and shifts to the west by 20° from 75 to 25 cb. A second trough can be seen over the Atlantic, sloping from 30°W at 75 cb to 65°W at 25 cb, again in the vicinity of a terrain-induced trough. It is worth noting also that, while the model tends to place the waves forced by the diabatic heating approximately in phase with those forced by the topography, the former have a somewhat smaller amplitude than the latter.

If we relate the forced waves of figure 11 to the smoothed diabatic heating distribution of figure 9B (dashed curve), we find that the troughs tend to occur near the regions of large-scale heating and the ridges consequently occur near the regions of large-scale cooling. These results agree qualitatively with those obtained by Smagorinsky (1953) and Gilchrist (1954) for winter conditions, using a single zonal wave number.

The response of the model to the forcing by both the topography and the diabatic heating appears in figure 12 as the dashed curve. The solid lines show how the observed heights, averaged between 30°N and 60°N, vary with longitude. We see that the model atmosphere is reasonably successful, especially at 75 cb, in reproducing the main features of the observed pressure surfaces. The dot-dashed curves in the figure are the computed heights with $F=6\times10^{-6}$ s^{-1} instead of 4×10^{-6} s^{-1}. The large friction coefficient reduces the amplitude and changes the position of the disturbances, but the effect is not drastic.

For both values of the friction coefficient, the troughs and ridges slope to the west with height and share this feature with the observed standing waves. The westward slope with height in the observed standing waves is not a peculiarity of January 1962, but rather seems to be the usual structure observed in January (e.g., Gilchrist 1954, Wiin-Nielsen 1961, Saltzman and Sankar-Rao 1963) and is therefore one feature that a model of the standing waves for January should be able to reproduce. We note that, with the present model, the systematic westward tilt was not present in the topographically induced perturbations (fig. 10) since one of the three major systems was sloping to the west, another was vertical, and the third was sloping to the east (with height). The westward tilt of the eddies in figure 12 is therefore due to the superposition of the thermally generated perturbations on those produced by the topography.

Figure 13 shows the standing waves forced by both the topography and the heating, using three different values of μ^2, namely, 0.324×10^{-12} m^{-2} (dot-dashed curve), 0.9×10^{-12} m^{-2} (dashed curve) and 1.5×10^{-12} m^{-2} (solid curve) corresponding to meridional wavelengths L_y of 100°, 60°, and 46° of latitude, respectively. The dashed curve of this figure is therefore the same as that of figure 12 and

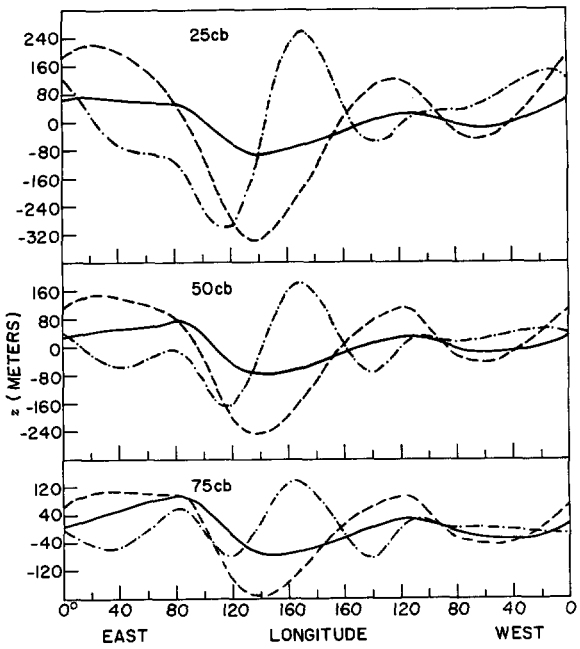

FIGURE 13.—Perturbation heights of the 25-, 50-, and 75-cb surfaces computed as a response to forcing by the topography and diabatic heating (with $N=18$) using $\mu^2=0.324 \times 10^{-12}$ m^{-2} (dot-dashed curves), 0.90×10^{-12} m^{-2} (dashed curves), and 1.50×10^{-12} m^{-2} (solid curves). The other parameters are the same as those in figure 1.

is reproduced here for convenience. While there is a substantial difference in amplitude of the response for $L_y=46°$ and 60° of latitude, the two sets of curves are very nearly in phase with each other and with the observed waves (fig. 12). The curves for $L_y=100°$ of latitude, on the other hand, differ appreciably from the others in the sense that they show a great deal more amplitude in the shorter zonal wavelengths, a result consistent with the discussion in sections 3 and 4, since an increase in L_y tends to push the quasi-resonance points to higher zonal wave numbers. We are led to the conclusion, then, from figures 12 and 13 that, among the three meridional wavelengths which we have used, $L_y=60°$ of latitude yields results that agree best with observations.

Some computations have also been made (see Derome 1968) to determine what improvements could be achieved by including more than one meridional mode in the perturbations and by considering the observed latitudinal dependence of the basic zonal wind in a β-plane channel bounded by solid walls at 30°N and 60°N. In such a channel, the maximum meridional half-wavelength of the perturbations is 30° of latitude and is equal to the single meridional half-wavelength used in figure 12. The resulting standing waves were found to be only slightly different from the computed ones shown in the above figure and are not reproduced here. It appears that the additional modes, in view of their very small meridional scale, are too far from the resonance point in parameter space to be of much significance. It was also found that the meridional variations in the basic zonal wind were not sufficiently large in these latitudes to be important. It is clear that, to represent properly the meridional structure of the perturbations and of the basic zonal wind, we must replace the β-plane approximation with the more natural spherical geometry; but this will not be attempted in this study.

In the following section, we shall use the β-plane approximation again to study the effects of allowing the friction coefficient F to be a function of longitude.

B. CASE OF A VARIABLE FRICTION COEFFICIENT

In addition to introducing zonal asymmetries in the ground elevation and diabatic heating, there is a third way in which the distribution of continents and oceans can have a bearing on the standing wave problem; and that is by causing a zonal asymmetry in the distribution of the friction coefficient. Unlike the topography and the diabatic heating, the zonal variation in F cannot, at least in the present formulation, interact directly with the zonal current to produce standing waves; but it *can* modify those created by the other two mechanisms. To study this effect, we shall again start with eq (12) and (13) and assume F to be a function of longitude only, so that eq (14) and (15) are still applicable. Upon substitution of the expansions (eq 14 and 15) into eq (12) and (13), the terms containing the variable coefficient $F(\lambda)$ are treated as follows. Let, for example,

$$F(\lambda)\hat{\psi}_*(\lambda)=\sum_{n=1}^{N}[g_n \cos(n\lambda)+h_n \sin(n\lambda)] \tag{30}$$

where

$$[g_n, h_n]=\frac{1}{\pi}\int_0^{2\pi} F(\lambda)\psi_*(\lambda)[\cos(n\lambda), \sin(n\lambda)]d\lambda. \tag{31}$$

Substituting the expansion (eq 15) for ψ_* with k as the index of summation into eq (31), we obtain

$$g_n=\sum_{k=1}^{N}(c_{k,n}A_k^*+e_{k,n}B_k^*) \tag{32}$$

and

$$h_n=\sum_{k=1}^{N}(j_{k,n}A_k^*+q_{k,n}B_k^*) \tag{33}$$

where

$$(c_{k,n}, e_{k,n})=\frac{1}{\pi}\int_0^{2\pi} F(\lambda)\cos(n\lambda)[\cos(k\lambda),\sin(k\lambda)]d\lambda \tag{34}$$

and

$$(j_{k,n}, q_{k,n})=\frac{1}{\pi}\int_0^{2\pi} F(\lambda)\sin(n\lambda)[\cos(k\lambda),\sin(k\lambda)]d\lambda. \tag{35}$$

Once $F(\lambda)$ is specified, the integrals in eq (34) and (35)

can be evaluated, at least numerically, so that the coefficients of A_k^* and B_k^* in eq (32) and (33) can be considered known. From eq (32) and (33), we also see that the coefficients g_n and h_n in eq (30) are simply linear combinations of the basic unknowns $A_1^*, \ldots, A_n^*$ and $B_1^*, \ldots, B_n^*$.

When one proceeds in this manner, the Fourier transforms of eq (12) and (13) can be written, after some elementary manipulations, as

$$(a_2+a_4)A_n^*-(a_3-a_5)A_n^T=qT_n, \tag{36}$$

$$(a_2+a_4)B_n^*-(a_3-a_5)B_n^T=-qQ_n, \tag{37}$$

$$(a_2+a_4)\sum_{k=1}^{N}(X_{k,n}A_k^*+Y_{k,n}B_k^*-1.6\,X_{k,n}A_k^T-1.6\,Y_{k,n}B_k^T)$$

$$-(a_2a_5+a_3a_4)A_n^T=(a_2+a_4)bR_n-a_2qT_n, \tag{38}$$

and

$$(a_2+a_4)\sum_{k=1}^{N}(Z_{k,n}A_k^*+W_{k,n}B_k^*-1.6\,Z_{k,n}A_k^T+1.6\,W_{k,n}B_k^T)$$

$$+(a_2a_5+a_3a_4)B_k^T=-(a_2+a_4)bS_n-a_2qQ_n \tag{39}$$

for $1\leq n\leq N$ where

$$(W_{k,n};X_{k,n};Y_{k,n};Z_{k,n})=r_k(e_{k,n};j_{k,n};q_{k,n};c_{k,n})$$

and

$$r_k=\frac{a\cos\varphi_0}{2nU_*^2}\left(\mu^2+\frac{k^2}{a^2\cos^2\varphi_0}\right).$$

The other symbols are as defined previously. We note that, from a mathematical standpoint, the cost of introducing a variable F consists of having to solve the above system of $4N$ equations in $4N$ unknowns rather than N distinct systems of four equations in four unknowns as was the case for a constant F.

Despite the rather complex nature of the system, eq (36–39), it is possible to deduce at least two properties of the eddies forced by the topography without solving the system of $4N$ equations explicitly. The first relates to the phase relationship between the $\hat{\psi}_*(\lambda)$ and $\hat{\psi}_T(\lambda)$ waves. It follows from eq (36) and (37) with $T_n=Q_n=0$ that

$$\frac{B_n^*}{A_n^*}=\frac{B_n^T}{A_n^T}. \tag{40}$$

The nth component of $\hat{\psi}_*$ is therefore either (1) exactly in phase or (2) exactly a half wavelength out of phase with the nth component of $\hat{\psi}_T$. This implies that, with the above formulation, no topographically induced standing wave can transport heat in the meridional direction, no matter what the zonal distribution of the friction coefficient may be.

It is also easy to show that the various Fourier components of the topographically induced stream function amplify or damp with height in a manner that is independent of $F(\lambda)$. The amplitude ratio A, defined as the ratio of the amplitudes of ψ_1 and ψ_3, that is,

$$A_n=\left[\frac{(A_n^*+A_n^T)^2+(B_n^*+B_n^T)^2}{(A_n^*-A_n^T)^2+(B_n^*-B_n^T)^2}\right]^{1/2},$$

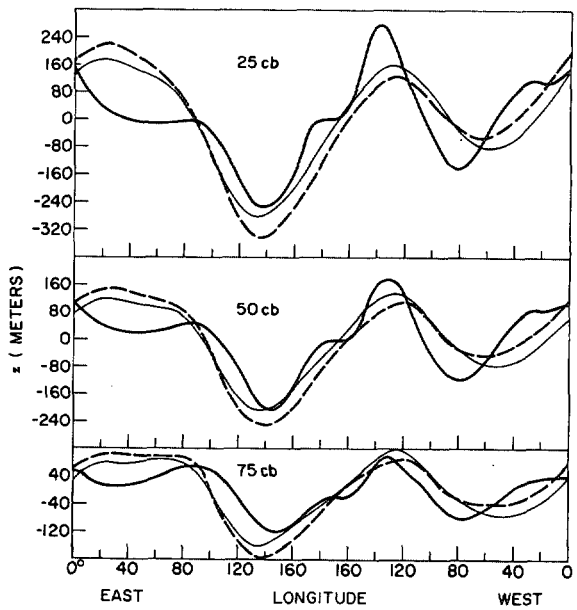

FIGURE 14.—Perturbation heights of the 25-, 50-, and 75-cb surfaces as they are observed (thick solid curves), computed as a response to forcing by topography and diabatic heating with $F_c/F_0=1$ (dashed curves), and computed as above but with $F_c/F_0=2$ (thin solid curves). The other parameters are the same as those in figure 1.

can be expressed, using eq (36) and (37) in the form

$$A_n=\left|\frac{a_2+a_3+a_4-a_5}{a_2-a_3+a_4+a_5}\right|$$

which is indeed independent of F. Figure 4 is therefore valid whether or not F is constant.

In the following, we shall prescribe a distribution of the friction coefficient and seek the solution to the system [eq (36–39)], using the surface topography and diabatic heating presented in subsection 5A. In view of our limited knowledge about $F(\lambda)$, we consider only simple cases in which $F=F_0$, a constant, over the oceans and $F=F_c$, another constant, over the continents. Thus we assume that the distribution

$$F=F_c \text{ for } 0<\lambda\leq 145°\text{E},$$

$$F=F_0 \text{ for } 145°\text{E}<\lambda\leq 120°\text{W},$$

$$F=F_c \text{ for } 120°\text{W}<\lambda\leq 60°\text{W},$$

and

$$F=F_0 \text{ for } 60°\text{W}<\lambda\leq 0$$

is sufficiently realistic for our purposes and consider three separate pairs (F_c, F_0, viz, $F_c/F_0=1$, 2, and 6), in each case keeping the zonal average of F equal to 4×10^{-6} s^{-1}. The same parameters as in figure 1 were used except for F and N, the latter being set equal to 10, although tests have shown that $N=5$ could have been used without appreciable effects on the results.

Figure 14 shows the heights of the 25-, 50- and 75-cb surfaces as functions of longitude for the cases $F_c/F_0=2$ (thin solid line) and F=const (dashed line) together

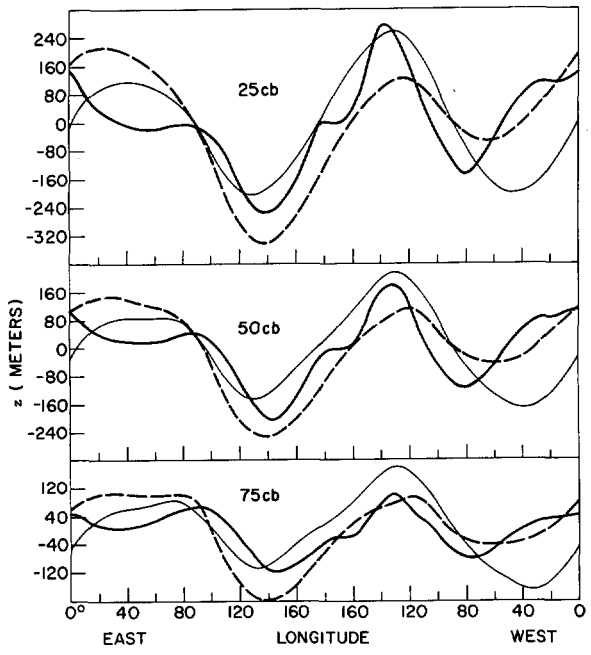

FIGURE 15.—Same as figure 14 except that the thin solid curves are computed with $F_c/F_0=6$.

with the observed heights averaged between 30°N and 60°N. Changing the distribution of the friction coefficient from F=const to $F_c/F_0=2$ has similar effects at all levels, namely, raising the height values from about 100°E eastward to 80°W and decreasing them over the rest of the domain. The effect is not drastic; but on the other hand, it should be noticed that the small changes are such as to bring the computed and observed standing waves into somewhat better agreement than in the case of a constant friction coefficient.

Figure 15 is similar to figure 14 except that its thin solid curves apply for $F_c/F_0=6$. The effects of the variations in F on the standing eddies are of the same general nature as those discussed above, but appreciably stronger.

We conclude from this section that, if the ratio $F_c/F_0=2$ is more nearly valid than the ratio $F_c/F_0=6$, the modifications effected by the variable F can be neglected in the standing wave problem; if the latter ratio is more appropriate than the former, however, the variations in F must be included.

6. CONCLUSIONS

This investigation has demonstrated that a two-level model of the atmosphere can be used to obtain considerable insight into the problem of the middle-latitude standing waves. It has been shown that, despite its extreme simplicity, the model possesses a large number of properties in common with some more elaborate, less easily analyzed models. Computations have also been made which indicate that the standing waves forced by the middle-latitude orography as obtained from Berkofsky and Bertoni (1955) tend to reinforce those produced by the heat sources obtained from Brown (1964) for January 1962 in the sense that the former are nearly in phase with the latter. The composite reponse of the model atmosphere to forcing by both topography and heating has been found to be in rather good agreement with the observed January 1962 standing eddies at 25, 50, and 75 cb when the meridional wavelength of the perturbations was taken to be 60° of latitude.

The extent to which the computed and observed stationary waves agree with each other can be interpreted as a measure of the quality of the modeling assumptions used here (e.g., linearization, single meridional scale, simplified distribution of the drag coefficient, neglect of the transient eddies). These were *not* embodied in Brown's computations of the heating field since, if we had used exactly the same modeling assumptions, the agreement between computations and observations would have been exact. In view of the rather good results obtained in this study, it can be concluded that the simplifying assumptions were reasonable as a first approximation.

Finally, it has been shown that the variation of the friction coefficient from an assumed constant value over the oceans to another constant value over the continents has only a small effect on the standing eddies when the ratio of these two values is taken to be 2; the effect, on the other hand, is quite large when the ratio is assumed to be 6.

While this study is similar to earlier studies in its basic formulation, it is novel in its application of observed heat sources and in the detailed analysis of the separate and combined effects of heating, topography, and friction. The agreement between the computed results and the observed state of the atmosphere is better than in earlier studies where more schematic heat sources were applied.

The main deficiency of this study is the use of β-plane geometry leading to unrealistic restrictions. Further studies should be aimed at removing these restrictions by adopting the less restrictive spherical geometry.

ACKNOWLEDGMENTS

This research was supported by NSF Grants GP-2561 and GA-841. The first author also wants to thank the Tecumseh Products Company and The University of Michigan for financial support.

REFERENCES

Berkofsky, Louis, and Bertoni, Eugene A., "Mean Topographic Charts for the Entire Earth," *Bulletin of the American Meteorological Society*, Vol. 36, No. 7, Sept. **1955**, pp. 350–354.

Bolin, Bert, "On the Influence of the Earth's Orography on the General Character of the Westerlies," *Tellus*, Vol. 2, No. 3, Stockholm, Sweden, Aug. **1950**, pp. 184–195.

Brown, John A., Jr., "A Diagnostic Study of the Tropospheric Diabatic Heating and the Generation of Available Potential Energy," *Tellus*, Vol. 16, No. 3, Stockholm, Sweden, Aug. **1964**, pp. 371–388.

Charney, Jule G., and Eliassen, A., "A Numerical Method for Predicting the Perturbations in the Middle-Latitude Westerlies," *Tellus*, Vol. 1, No. 2, Stockholm, Sweden, May **1949**, pp. 38–54.

Derome, Jacques F., "The Maintenance of the Time-Averaged State of the Atmosphere," Ph. D. thesis, Department of Meteorology and Oceanography, The University of Michigan, Ann Arbor, July **1968**, 129 pp.

Döös, Bo R., "The Influence of Exchange of Sensible Heat With the Earth's Surface on the Planetary Flow," *Tellus*, Vol. 14, No. 2, Stockholm, Sweden, May **1962**, pp. 133–147.

Gambo, Kanzaburo, "The Topographical Effect Upon the Jet Stream in the Westerlies," *Journal of the Meteorological Society of Japan*, Ser. 2, Vol. 34, No. 1, Tokyo, Mar. **1956**, pp. 24–28.

Gilchrist, Bruce, "The Seasonal Phase Changes of Thermally Produced Perturbations in the Westerlies," *Proceedings of the Toronto Meteorological Conference, Toronto, Canada, September 9–15, 1953*, American Meteorological Society and Royal Meteorological Society, Boston, Mass., **1954**, pp. 129–131.

Mintz, Yale, "Very Long-Term Global Integration of the Primitive Equations of Atmospheric Motion," *World Meteorological Organization Technical Note* No. 66, Geneva, Switzerland, **1965**, pp. 141–167.

Miyakoda, Kikuro, Smagorinsky, Joseph, Strickler, Robert F., and Hembree G. D., "Experimental Extended Predictions With a Nine-Level Hemispheric Model," *Monthly Weather Review*, Vol. 97, No. 1, Jan. **1969**, pp. 1–76.

Murakami, Takio, "The Topographic Effects in the Three-Level Model of the s-Coordinate," *Papers in Meteorology and Geophysics*, Vol. 14, No. 3–4, Tokyo Meteorological Research Institute, Japan, Dec. **1963**, pp. 144–150.

Phillips, Norman A., "The General Circulation of the Atmosphere: A Numerical Experiment," *Quarterly Journal of the Royal Meteorological Society*, Vol. 82, No. 352, London, England, Apr. **1956**, pp. 123–164.

Phillips, Norman A., "Geostrophic Errors in Predicting the Appalachian Storm of November 1950," *Geophysica*, Vol. 6, No. 3–4, Helsinki, Finland, **1958**, pp. 389–405.

Phillips, Norman A., "Geostrophic Motion," *Reviews of Geophysics*, Vol. 1, No. 2, May **1963**, pp. 123–176.

Saltzman, Barry, "Perturbation Equations for the Time-Averaged State of the Atmosphere Including the Effects of Transient Disturbances," *Geofisica Pura e Applicata*, Vol. 48, No. 1, Milan, Italy, **1961**, pp. 143–150.

Saltzman, Barry, "On the Theory of the Winter-Average Perturbations in the Troposphere and Stratosphere," *Monthly Weather Review*, Vol. 93, No. 4, Apr. **1965**, pp. 195–211.

Saltzman, Barry, "Surface Boundary Effects on the General Circulation and Macroclimate: A Review of the Theory of the Quasi-Stationary Perturbations in the Atmosphere," *Meteorological Monographs*, Vol. 8, No. 30, American Meteorological Society, Boston, Mass., Feb. **1968**, pp. 4–19.

Saltzman, Barry, and Sankar-Rao, M., "A Diagnostic Study of the Mean State of the Atmosphere," *Journal of the Atmospheric Sciences*, Vol. 20, No. 5, Sept. **1963**, pp. 438–447.

Sankar-Rao, M., "Continental Elevation Influence on the Stationary Harmonics of the Atmospheric Motion," *Pure and Applied Geophysics*, Vol. 60, No. 1, Basel, Switzerland, **1965***a*, pp. 141–159.

Sankar-Rao, M., "Finite Difference Models for the Stationary Harmonics of Atmospheric Motion," *Monthly Weather Review*, Vol. 93, No. 4, Apr. **1965***b*, pp. 213–224.

Sankar-Rao, M., "On the Influence of the Vertical Distribution of Stationary Heat Sources and Sinks in the Atmosphere," *Monthly Weather Review*, Vol. 93, No. 7, July **1965***c*, pp. 417–420.

Sankar-Rao, M., and Saltzman, Barry, "On a Steady State Theory of Global Monsoons," *Tellus*, Vol. 21, No. 3, Stockholm, Sweden, Aug. **1969**, pp. 308–330.

Smagorinsky, Joseph, "The Dynamical Influence of Large-Scale Heat Sources and Sinks on the Quasi-Stationary Mean Motions of the Atmosphere," *Quarterly Journal of the Royal Meteorological Society*, Vol. 79, No. 341, London, England, July **1953**, pp. 342–366.

Smagorinsky, Joseph, "General Circulation Experiments With the Primitive Equations: I. The Basic Experiment," *Monthly Weather Review*, Vol. 91, No. 3, Mar. **1963**, pp. 99–164.

Staff Members, Academia Sinica, Institute of Geophysics and Meteorology, Peking, China, "On the General Circulation Over Eastern Asia, Pt. 3," *Tellus*, Vol. 10, No. 3, Stockholm, Sweden, Aug. **1958**, pp. 299–312.

Thompson, Philip Duncan, *Numerical Weather Analysis and Prediction*, The Macmillan Co., Inc., New York, N.Y., **1961**, 170 pp.

Wiin-Nielsen, Aksel, "On Certain Integral Constraints for the Time Integration of Baroclinic Models," *Tellus*, Vol. 11, No. 1, Stockholm, Sweden, Feb. **1959**, pp. 45–59.

Wiin-Nielsen, Aksel, "On the Distribution of Temperature Relative to Height in Stationary Planetary Waves," *Tellus*, Vol. 13, No. 2, Stockholm, Sweden, May **1961**, pp. 127–139.

[*Received May 27, 1970; revised September 13, 1970*]